THE JOURNAL OF BIOLOGICAL CHEMISTRY
Vol. 280, No. 6, Issue of February 11, pp. 4649–4655, 2005
Printed in U.S.A.
© 2005 by The American Society for Biochemistry and Molecular Biology, Inc.

Activation of Ataxia Telangiectasia Mutated by DNA Strand Break-inducing Agents Correlates Closely with the Number of DNA Double Strand Breaks*

Received for publication, October 12, 2004, and in revised form, November 15, 2004
Published, JBC Papers in Press, November 15, 2004, DOI 10.1074/jbc.M411588200

Ismail Hassan Ismail‡, Susanne Nyström‡, Jonas Nygren§, and Ola Hammarsten‡¶

From the ‡Department of Clinical Chemistry and Transfusion Medicine, Sahlgrenska University Hospital, Göteborg University, SE-413 45 Göteborg, Sweden and §Laboratory of Molecular and Cellular Toxicology, Department of Industrial Hygiene and Toxicology, Finnish Institute of Occupational Health, Topeliuksenkatu 41aA, FIN-00250 Helsinki, Finland

The protein kinase ataxia telangiectasia mutated (ATM) is activated when cells are exposed to ionizing radiation (IR). It has been assumed that ATM is specifically activated by the few induced DNA double strand breaks (DSBs), although little direct evidence for this assumption has been presented. DSBs constitute only a few percent of the IR-induced DNA damage, whereas the more frequent single strand DNA breaks (SSBs) and base damage account for over 98% of the overall DNA damage. It is therefore unclear whether DSBs are the only IR-induced DNA lesions that activate ATM. To test directly whether or not DSBs are responsible for ATM activation, we exposed cells to drugs and radiation that produce different numbers of DSBs and SSBs. We determined the resulting ATM activation by measuring the amount of phosphorylated Chk2 and the numbers of SSBs and DSBs in the same cells after short incubation periods. We found a strong correlation between the number of DSBs and ATM activation but no correlation with the number of SSBs. In fact, hydrogen peroxide, which, similar to IR, induces DNA damage through hydroxyl radicals but fails to induce DSBs, did not activate ATM. In contrast, we found that calicheamicin-induced strand breaks activated ATM more efficiently than IR and that ATM activation correlated with the relative DSB induction by these agents. Our data indicate that ATM is specifically activated by IR-induced DSBs, with little or no contribution from SSBs and other types of DNA damage. These findings have implications for how ATM might recognize DSBs in cells.

DNA double strand breaks (DSBs)[1] are the most toxic form of DNA damage, because a single unrepaired DSB can lead to losses of large pieces of DNA during mitosis. Therefore, cells have evolved effective pathways for the repair and detection of DSBs (reviewed in Ref. 1). DSBs are generated by ionizing radiation (IR) and drugs that produce radicals or interfere with topoisomerase II function. It has been shown for IR that the few DSBs that are produced correlate closely to the amount of cell death that occurs, whereas the 100-fold more abundant single strand DNA breaks (SSBs) and base damage are probably of minor importance in relation to the cytotoxic effect (2).

ATM is a protein serine/threonine kinase activated in cells exposed to IR (3–5). ATM activation results in rapid induction of numerous cell responses, which leads to activation of cell cycle checkpoints (1). Cells without ATM function show a profound defective response to IR and are therefore radiosensitive. They are able to repair most, but not all, IR-induced DNA damage (6). The ATM gene is mutated in ataxia telangiectasia (7), a pleiotropic recessive human disorder characterized by cerebellar degeneration, immunodeficiency, cancer predisposition, and extreme radiosensitivity (reviewed in Refs. 8 and 9). ATM phosphorylates and controls several signaling pathways that are activated by IR. Important examples are the p53 protein, which mediates the G_1/S checkpoint, and Chk2, which activates the G_2/M checkpoint by inhibiting the CDC25 phosphatase (1, 10). Among the ATM substrates involved in DNA damage recognition are serine 139 of histone 2AX (H2AX) (11), threonine 68 of Chk2 (12–14), and serine 957 of SMC1 (15). ATM also phosphorylates and regulates several proteins involved in the response to IR, the functions of which are still unknown. Examples are the Brca1 and Nbs1, proteins mutated in the human cancer disorders, hereditary breast cancer, and AT-like disorder (reviewed in Ref. 1).

A recent report indicates that ATM is an inactive multimer in cells. In response to IR, ATM phosphorylates itself to become an active monomer capable of phosphorylating downstream targets, such as p53 (16). However, purified ATM and ATM in crude cell extract do not change their molecular weight in response to phosphorylation, which indicates that the multimeric form could be unstable or dependent on, as yet, unknown factors inside the cell (17). ATM activation in response to IR is dependent on the function of Mre11, Rad50, and Nbs1, which form a functional complex with helicase and nuclease activities (MRN complex) (18, 19). Mre11 can interact with ATM in a purified system and stimulate ATM kinase activity (20). However, the kinase activity observed in preparations of ATM alone or together with the MRN complex is not specifically stimulated by DNA ends (17, 20, 21). In addition, several reports indicate that purified ATM binds poorly to DNA (17, 21). Our knowledge of how ATM is activated by IR is thus incomplete.

Despite the profound importance of ATM in cellular response to IR, we still do not know what type of DNA damage is recog-

* This work was supported by the Swedish Cancer Society, Swedish Research Council, King Gustav V Jubilee Clinic Cancer Research Foundation, and the Sahlgrenska University Hospital Research Foundation. The costs of publication of this article were defrayed in part by the payment of page charges. This article must therefore be hereby marked "*advertisement*" in accordance with 18 U.S.C. Section 1734 solely to indicate this fact.

¶ To whom correspondence should be addressed. Tel.: 46-31-3421561; Fax: 46-31-828458; E-mail: ola.hammarsten@clinchem.gu.se.

[1] The abbreviations used are: DSB, DNA double strand break; SSB, single strand break; TSB, total strand break (DSB+SSB); IR, ionizing radiation; DNA-PK, DNA-dependent protein kinase; DNA-PKcs, the catalytic subunit of DNA-PK; AT, ataxia telangiectasia; ATM, ataxia telangiectasia mutated; PBS, phosphate-buffered saline; PAR, poly-(ADP-ribose); PARP, poly(ADP-ribose) polymerase; FAR, fraction of activity released; CLM, calicheamicin γ1; MRN complex, Mre11, Rad50, and Nbs1.

This paper is available on line at http://www.jbc.org
This is an open access article under the CC BY license.

nized by ATM. It has been assumed that ATM is activated by the few DSBs induced by IR or topoisomerase II toxins. However, there is no direct data indicating that DSBs are the only initiating event. One problem is that the majority of IR-induced DNA damage are SSBs and base damage. Only 1–2% of the DNA damage is DSBs. For topoisomerase II toxins, a recent report indicates that most of the lesions produced by these drugs are topoisomerase II-linked SSBs (22). This implies the possibility that ATM is also capable of detecting other types of DNA damage, such as base damage induced by UV light (23, 24) and hexavalent chromium compounds that fail to induce quantifiable numbers of DSBs (25). Moreover, single strand oligonucleotides have been shown to induce ATM/p53-dependent apoptosis (26). It has recently been proposed that the local chromatin relaxation that occurs around a DSB is the activation signal for ATM rather than the actual DSB (16). In favor of the chromatin relaxation model, it has been shown that ATM can be activated by a series of compounds and hypotonic treatments that induce chromatin alteration in the apparent absence of DNA damage (16). One potential problem with the chromatin relaxation model is that SSBs would possibly be able to activate ATM, because SSBs and DSBs are both capable of relaxing supercoiled DNA. In fact, by measuring psoralen intercalation efficiency, it has been shown that IR-induced SSBs effectively abolish chromatin supercoiling in mammalian cells (27, 28). SSBs should therefore be able to activate ATM to some extent.

To test directly whether or not ATM is activated specifically by DSBs, we induced strand breaks in cellular DNA with compounds and radiation that produce different numbers of DSBs and SSBs. We measured ATM activation and the number of SSBs and DSBs in the treated cells after short incubation periods to prevent secondary events. We found that ATM is not activated at all in response to SSBs, even at numbers that would be able to fully relax chromatin supercoiling. In addition, we also found that the number of DSBs correlates closely with the ATM activity in the cells, whereas no correlation was found with the number of SSBs. Our data indicate that ATM is directly activated by the few DSBs that are introduced by IR.

MATERIALS AND METHODS

Cells and Reagents—Calicheamicin γ1 (CLM) was a generous gift from Prof. George Ellestad (Wyeth-Ayers Research). The drug was dissolved at 2 mM in Me_2SO and stored at −70 °C. Epstein-Barr virus-immortalized normal (catalog number GM02254) and AT (catalog number GM01526) human lymphoblast cultures were obtained from the Coriell Institute for Medical Research. All lymphoblast cells were cultured in RPMI 1640 medium (Invitrogen) supplemented with 10% fetal bovine serum and 100 nM glutamine and penicillin/streptomycin in a humidified atmosphere with 5% CO_2.

Measurement of ATM Activation—H2AX phosphorylation was measured in cells treated with the DNA-damaging agents for 15 min at 37 °C (as indicated in Fig. 4*C*). After washing with cold PBS, the cells were suspended in cell lysis buffer, and H2AX phosphorylation was measured as described previously (29). Chk2, SMC1, and ATM autophosphorylation were measured in human lymphoblast cells treated for 15 min at 37 °C with the indicated drugs (see Fig. 4). The cells were lysed in 20 mM Tris-HCl buffer, pH 8.0, containing 100 mM NaCl, 0.5% Triton X-100, 10 mM NaF, 1 mM Na_3VO_4, 2 mg/ml aprotinin, 2 mg/ml leupeptin, 2 mg/ml antipain and 1 mM phenylmethylsulfonyl fluoride for 15 min on ice. The cell extract was clarified by centrifugation at 12,000 revolutions/min for 10 min at 4 °C and separated on 10% SDS-polyacrylamide gel. After transfer to nitrocellulose membranes (Amersham Biosciences), the membranes were blocked with Blotto (5% nonfat dry milk and 0.1% Tween 20 in PBS) and incubated with a polyclonal antibody specific to Chk2 phosphorylated at Thr-68 (Cell Signaling Technology), SMC1 phosphorylated at Ser-957 (Bethyl Laboratories), or ATM phosphorylated at Ser-1981 (Rockland). After incubation with a secondary antibody, the membranes were developed using enhanced chemiluminescence (SuperSignal® West Dura extended duration substrate, Pierce). After stripping with 50 mM glycine, pH 2.3, for 30 min, the membranes were blocked and reprobed with a Ku70 antibody (Novagene) to show equal loading.

Measurement of Poly(ADP-ribose) (PAR) Polymerase (PARP) Activation in Cells—For detection of PAR, cells were harvested, washed with PBS, and treated on ice with different concentrations of H_2O_2, as indicated in Fig. 5*B*. After treatment, the cells were incubated for 15 min at 37 °C. The cell extracts were then prepared by adding SDS-PAGE sample buffer (1% SDS, 1% β-mercaptoethanol, 5% glycerol, 25 mM Tris-HCl, pH 6.5, and 0.05% bromphenol blue) to each sample. The samples were separated on SDS-PAGE and subsequently transferred to nitrocellulose membranes. To detect PAR bound to proteins, the membrane was probed with a monoclonal antibody to PAR (1:500 dilution; Trevigen) and peroxidase-labeled goat antibody to mouse IgG (Sigma). The bands were quantified with ChemiDoc (Bio-Rad) using the Quantity One software.

Fraction of Activity Released (FAR) Assay—The number of DSBs in cells treated with IR, CLM, or H_2O_2 were monitored with the FAR assay (29). After exposure to drugs or radiation, the cells were kept on ice at all times, and all solutions added to the cells were ice-cold. The cells were centrifuged, resuspended in PBS supplemented with 0.2 mg/ml sheared herring sperm DNA and 56 mM β-mercaptoethanol to inactivate excess CLM, and incubated on ice for 5 min. The cells were then washed with PBS, and 150,000 cells were mixed with melted agarose (1.25% type VII in PBS with 5 mM EDTA) and transferred to a plug mold. The cells in the plug were then lysed at 4 °C for a minimum of 24 h in lysis buffer (25 mM EDTA, pH 8.5, 0.5% SDS, 3 mg/ml proteinase K added just prior to lysis). Longer incubation times did not alter the quality of the data. The cells were then resolved using agarose gel electrophoresis (0.7%) in 1× TAE (0.04 M Tris acetate, 1 mM EDTA, pH 8) at 4 °C for 17 h at 2 V/cm. The relative amount of cellular DNA migrating into the gel (FAR) was quantified using laser scanning equipment (Typhoon 9200 Variable Mode Imager, ImageQuant 5.2) to calculate the number of DSBs.

Comet Assay—The comet assay was performed as described previously (29) with some modifications. Briefly, 5,000–10,000 cells were mixed with 150 μl of 0.75% low melting agarose (type VII, Sigma) kept at 37 °C. The agarose-cell suspension was spread onto prechilled gel bond film (Cambrex Bio Science). The preparations were left on a chilled plate for 5 min before lysis (0.03 M NaOH, 1 M NaCl, 2 mM EDTA, 0.5% *N*-lauryl sarcosine) for 1 h and thereafter equilibrated (0.03 M NaOH, 2 mM EDTA) for 1 h. Electrophoresis of the agarose-imbedded cells was run at 0.67 V/cm for 15 min in the same solution. The film was then neutralized in 0.4 M Tris-HCl, pH 7.5. The film was fixed in absolute ethanol for 2 h and allowed to dry. After staining the film with SybrGold (Molecular Probes) for 5 min, it was rinsed briefly in deionized water. Analysis of the DNA that migrated from the nuclei, the tail moment, was done using an Olympus fluorescence microscope aided by the Kinetic Imaging Komet II system.

Immunofluorescence Microscopy—For immunofluorescence experiments, cells were concentrated by centrifugation onto microscopic slides (cytospin), fixed in 3.7% paraformaldehyde supplemented with 20% sucrose for 15 min at room temperature, and permeabilized in 0.1% Triton X-100 in PBS. The fixed cells were blocked for 1 h in 10% (v/v) serum in PBS at 37 °C and rinsed with PBS. Mouse monoclonal anti-PAR antibody (Trevigen) was diluted 1:1000 in blocking buffer and incubated with the cells for 1 h at 37 °C. Alexa Fluor™ 594 goat anti-mouse secondary antibody (Molecular Probes) was diluted 1:4000 and incubated with the cells for 1 h at 37 °C, protected from light. The cells were counterstained with 0.1 μg/ml 4′,6-diamidino-2-phenylindole in Prolong® Gold antifade reagent (Molecular Probes). Confocal fluorescence images were captured using a Zeiss LSM510 laser scanning microscope (Zeiss, Inc.). Images were obtained in 8-bit mode. The fluorescence intensities were placed within the linear range of the detector by setting the amplifier offset to zero. The detector gain was adjusted so that the peak intensities never reached saturation levels.

RESULTS

Measurement of ATM Kinase Activity—To be able to specifically measure ATM kinase activity in cells, we screened several commercially available phosphospecific antibodies against known ATM substrates using immunoblot. We noted that all ATM substrates were phosphorylated in a DNA damage-dependent manner in AT cells (Fig. 1*A*), indicating that other kinases can be substituted for ATM (30). However, at low DNA damage levels and at short times after induction of DNA damage, Chk2, SMC1, and H2AX were almost exclu-

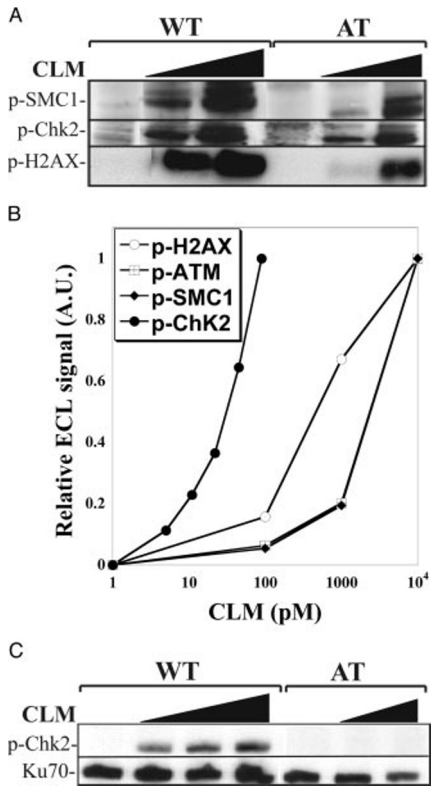

FIG. 1. **Measurement of ATM kinase activity in cells.** *A*, human lymphoblast cells from wild type (*WT*) and AT patients (*AT*) were treated with 0, 1, or 10 nM CLM for 30 min at 37 °C, and the extracts were analyzed using immunoblot. Immunoblots were probed using phosphospecific antibodies, as indicated in the figure. *B*, human wild type lymphoblast cells treated with different concentrations of CLM, as indicated in the figure, for 15 min at 37 °C and then analyzed using immunoblot. Immunoblots were quantified with ChemiDoc (Bio-Rad) using Quantity One software, and values were plotted, as shown in the figure, on a log scale. *C*, human lymphoblast cells from wild type and AT patients were treated with 0, 0.1, 0.3, and 1 nM CLM for 15 min at 37 °C. The immunoblot was stained with an antibody against phospho-Chk2. After stripping, the membrane was reprobed with Ku70 antibody to show equal loading. *A.U.*, arbitrary units.

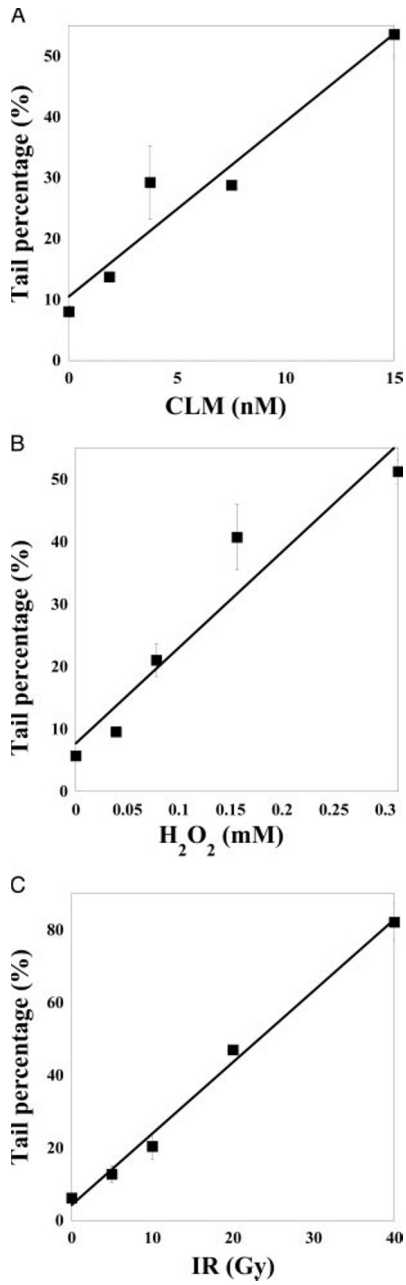

FIG. 2. **DNA strand break induction in WT cells by H_2O_2, CLM, and IR, measured with the Comet assay.** Cells were treated with different concentrations of CLM (*A*), H_2O_2 (*B*), or IR (*C*) for 15 min at 37 °C and analyzed using the comet assay. *Gy*, gray.

sively phosphorylated in normal B cells. We also compared the relative strengths of the signals from the ATM substrates in immunoblot analysis. We found that with a 15-min incubation period, Chk2 phosphorylation could be detected at 10-fold lower concentrations of the DSB-inducing drug CLM as compared with SMC1, H2AX, and ATM autophosphorylation (Fig. 1*B*). We therefore optimized the incubation time and DNA damage levels for the Chk2 phosphorylation in all subsequent experiments so that no phosphorylation of Chk2 was detected in AT cells, thus allowing us to specifically measure ATM activation in cells (Fig. 1*C*).

Measurement of H_2O_2-, IR-, and CLM-induced Strand Breaks—To study the possible involvement of SSBs, DNA base damage, or chromatin relaxation in ATM kinase activation, we induced DNA strand breaks with drugs and radiation that produced different numbers of DSBs and SSBs. Hydrogen peroxide (H_2O_2) induces predominantly SSBs by production of randomly distributed hydroxyl radicals (31–33). IR also induces DNA strand breaks by production of hydroxyl radicals when the photons react with water. However, because multiple hydroxyl radicals are produced in close proximity, some of the events result in DSBs. Apart from this difference, the DNA damage distribution and the chemistry of the DNA lesions produced by H_2O_2 and IR are very similar (33–35). CLM is an enediyne antibiotic that binds and cleaves DNA by cooperative activation of two radical centers in the molecule. Because the two radical centers become positioned close to the opposite strands in the DNA, a large proportion of the strand breaks produced are DSBs (36).

To measure the relative number of DSBs and SSBs produced by these agents, we first exposed B cells to different concentrations of drugs and different doses of IR. Cells from each treatment were then subjected to analysis of total DNA strand breaks (TSBs = SSBs + DSBs) using the alkaline comet assay and DSBs using the FAR assay. The results showed that, although all of these agents effectively induced strand breaks as measured using the comet assay (Fig. 2), only IR and CLM were able to induce DSBs as measured using the FAR assay (Fig. 3). The cells treated with H_2O_2 did not show any DSBs in this assay, in agreement with previous findings (37). To further explore this, we extended the H_2O_2 titration to 3 mM. At these concentrations of H_2O_2, all DNA migrated out from the nuclei

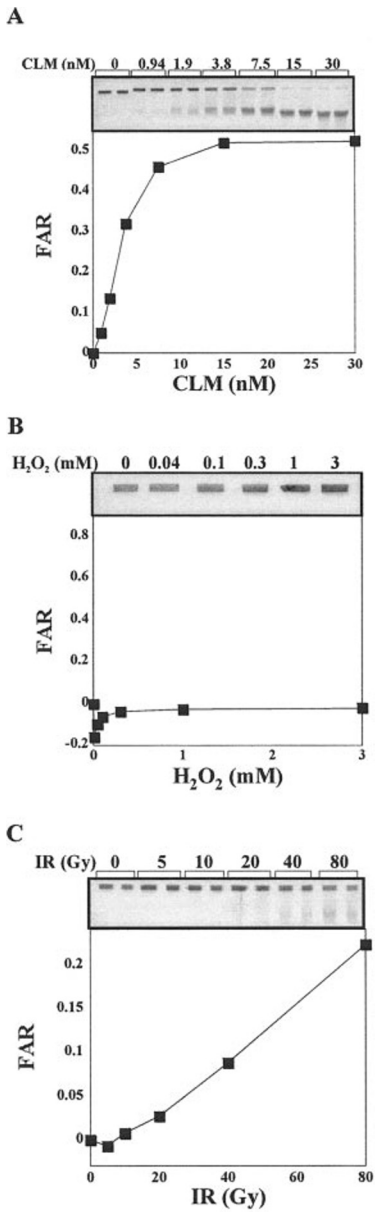

FIG. 3. **DSB induction in WT cells by H_2O_2, CLM, and IR, measured with the FAR assay.** *A*, β cells treated with different concentrations of CLM (0–30 nM) (*A*), H_2O_2 (0–3 mM) (*B*), or IR (0–80 gray) (*C*), incubated for 15 min at 37 °C, and then analyzed using the FAR assay. The amount of DNA entering the gel (the FAR value) was quantified and used to generate the graphs. *Gy*, gray.

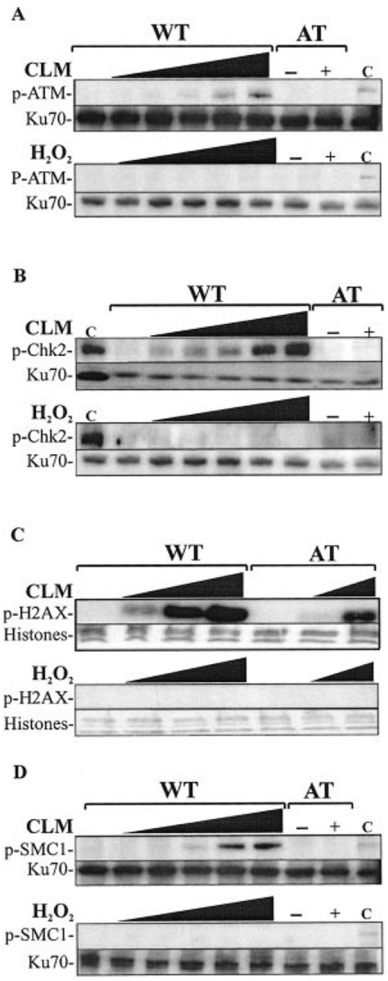

FIG. 4. **The cellular DNA damage response induced by CLM and H_2O_2.** Human lymphoblast cells from wild type (*WT*) and AT patients (*AT*) were treated with different concentrations of CLM (0, 0.001, 0.01, 0.1, 1, and 10 nM) or H_2O_2 (0, 0.3125, 0.625, 1.25, 2.5, and 5 mM) at 37 °C for 15 min. Human wild type lymphoblast cells treated with 10 nM CLM for 30 min at 37 °C were used as a control (*c*). The different ATM-dependent phosphorylations were measured by immunoblot using phosphospecific antibodies. *A*, immunoblot using phospho-ATM antibody. *B*, immunoblot using phospho-Chk2 antibody. *C*, immunoblot using phospho-H2AX antibody. *D*, immunoblot using phospho-SMC1 antibody. Lower concentrations of CLM (1, 5, 11, 22, 45, 90 pM) were used in the phospho-Chk2 immunoblot.

in the comet assay, preventing any calculation of the number of TSBs. However, by extrapolating the strand breaks from measurements done at 0.2 mM and assuming a linear dose-response relationship, we concluded that over 400,000 SSBs/cell were produced at 3 mM H_2O_2. This number corresponds to one SSB for every 6000 bp. Despite the large number of strand breaks, no DSBs were observed in the FAR assay (Fig. 3*B*). From the detection limit of DSBs in the FAR assay and the TSBs produced at 3 mM H_2O_2, we estimated that <0.1% of all DNA strand breaks induced by H_2O_2 are DSBs. The percentages of DSBs were ~30% for CLM and 5% for IR, based on our previous results (29).

H_2O_2-induced DNA Damage Fails to Activate ATM—We wanted to know whether ATM was activated in cells treated with H_2O_2. We therefore measured the phosphorylation of known ATM targets using immunoblot with phosphospecific antibodies in extracts from the same batch of cells analyzed for TSBs and DSBs. Measurements of ATM activation was done at 15 min after the addition of the drug to prevent secondary events. As a control, we also measured ATM activation in cells treated with CLM. We found that H_2O_2 failed to induce any detectable phosphorylation of the ATM substrates (Fig. 4). In contrast, CLM induced strongly dose-dependent phosphorylation of SMC1, ATM, H2AX, and Chk2 (Fig. 4). It was possible that the large amount of oxidative damage produced by H_2O_2 might result in inactivation of many processes in the cell, including ATM kinase activity. To determine whether the cells were able to respond to the SSBs induced by H_2O_2, we measured PAR modification of proteins in the cells after H_2O_2 treatment. PAR is added to the proteins by the PAR polymerases (PARPs) in response to SSBs (38). Using immunofluorescence, we found a strong nuclear PAR response in cells treated with both 0.5 and 5 mM H_2O_2 (Fig. 5*A*). Using immunoblot with the same PAR-specific antibody, we found that H_2O_2 stimulated PARP activity with a linear dose-response relationship up to 1 mM, indicating that the cells were able to recognize the SSBs produced. However, at 3 mM, the linear dose-response relation-

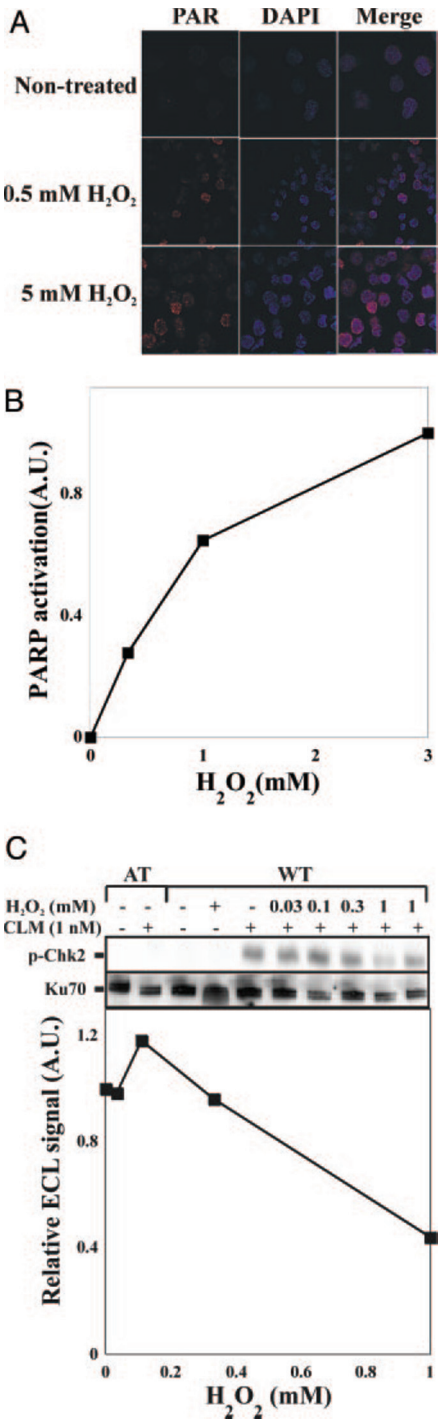

FIG. 5. **H_2O_2-induced strand breaks trigger PARP activation.** Poly(ADP-ribose) (*PAR*) measured in WT cells treated with the concentrations of H_2O_2 indicated in the figure at 37 °C for 15 min. PARP activation was monitored with either immunoblot or immunofluorescence using antibody against PAR. *A*, immunofluorescence on cells treated with H_2O_2. *B*, the ECL signal from the immunoblot was quantified using a ChemiDoc and plotted as shown in the figure. *C*, inactivation of ATM by H_2O_2. WT cells were treated with 1 nM CLM on ice for 30 min before the addition of different concentrations of H_2O_2, incubated at 37 °C for 15 min, and phospho-Chk2 measured with immunoblot. *Lane 1*, untreated AT cells. *Lane 2*, AT cells treated with 1 nM CLM. *Lane 3*, untreated WT cells. *Lane 4*, WT cells treated with 1 mM H_2O_2. *Lane 5*, WT cells treated with 1 nM CLM. *Lanes 6–9*, WT cells were treated with 1 nM CLM for 30 min on ice before the addition of different concentrations of H_2O_2, as indicated in the figure. The cells were subsequently incubated at 37 °C for 15 min. *Lane 10*, CLM and H_2O_2 were added simultaneously to WT cells and incubated on ice for 30 min before further incubation at 37 °C for 15 min. The ECL signal from the blot was quantified using a ChemiDoc and plotted (*lower panel*). *DAPI*, 4′,6-diamidino-2-phenylindole. *A.U.*, arbitrary units.

ship was lost. Apparently, PARP activity was partially inhibited at this concentration (Fig. 5*B*).

We also tested whether or not ATM was inhibited by H_2O_2 by first introducing DSBs with a fixed concentration of CLM (1 nM). This pretreatment was done on ice to prevent any ATM activation. We then added different concentrations of H_2O_2 and incubated the cells at 37 °C for 15 min to allow the ATM to become activated. We found that 1 mM H_2O_2 reduced ATM activation by 50%, whereas concentrations below 0.3 mM did not affect the ATM activity (Fig. 5*C*). Similar results were obtained using IR-induced DSBs before H_2O_2 treatment (data not shown). The failure to observe ATM activation in response to 0.3 mM H_2O_2 could therefore not be attributed to ATM inhibition by H_2O_2. In addition, these data indicate that experiments at H_2O_2 concentrations >1 mM would not be informative, because ATM would be partially inactivated. We concluded that ATM was not activated by H_2O_2-induced DNA damage, because no DSBs were formed.

ATM Activation by CLM and IR Correlates with the Number of DSBs—We then compared ATM activation after CLM- and IR-induced DNA damage. CLM is one of the most effective DSB-inducing agents known. In fact, 30% of all DNA strand breaks are DSBs. In contrast, most of the IR-induced DNA strand breaks are SSBs, and only 2–5% of the strand breaks are DSBs (29). If ATM is exclusively activated by DSBs, it is therefore expected that ATM would be activated to a higher extent by CLM-induced DNA strand breaks than by IR-induced DNA strand breaks. We therefore measured Chk2 phosphorylation in the same CLM- or IR-treated cells used for TSB and DSB determination. We found dose-dependent induction of Chk2 phosphorylation for both IR- and CLM-treated cells. In parallel experiments, no Chk2 phosphorylation was observed in AT cells, indicating that all Chk2 phosphorylation was attributable to ATM kinase activity (Fig. 6, *A* and *B*). In these experiments, we also included an extra sample from CLM-treated cells to serve as an internal control. We used this internal control to normalize Chk2 phosphorylation to be able to compare the Chk2 phosphorylation in the individual experiments (Fig. 6, *A* and *B*). We then plotted the Chk2 phosphorylation against the number of TSBs determined using the comet assay. The results showed that CLM-induced strand breaks activated ATM to a higher extent than did IR. By comparing the relative Chk2 phosphorylation in these experiments, we calculated that CLM-induced TSBs activated ATM five times better than IR-induced TSBs (Fig. 6*C*). Because the difference in DSB induction between CLM and IR is 5-fold (30% for CLM *versus* 5% for IR), these data fit closely with the expectation that DSBs activate ATM and that other types of DNA damage contribute little if anything to the ATM activation observed in IR-treated cells.

DISCUSSION

ATM is central to the cellular response to IR and phosphorylates several key proteins, such as Chk2 and p53, resulting in cell cycle arrest. Although it has been assumed that the few DSBs induced by IR are solely responsible for ATM activation, little direct evidence of this assumption has been presented.

The aim of this study was to determine whether it is SSBs or other types of IR-induced DNA damage that contribute to ATM activation. We therefore compared the activation of ATM in response to IR with activation on the basis of two unrelated drugs that induce different numbers of SSBs and DSBs. We measured ATM activation, TSBs, and the number of DSBs in the same cell population. We also carefully validated the assay used to measure ATM activation and used short incubation periods to avoid contributions from secondary events. We found that SSBs induced by H_2O_2 failed to activate ATM, even at

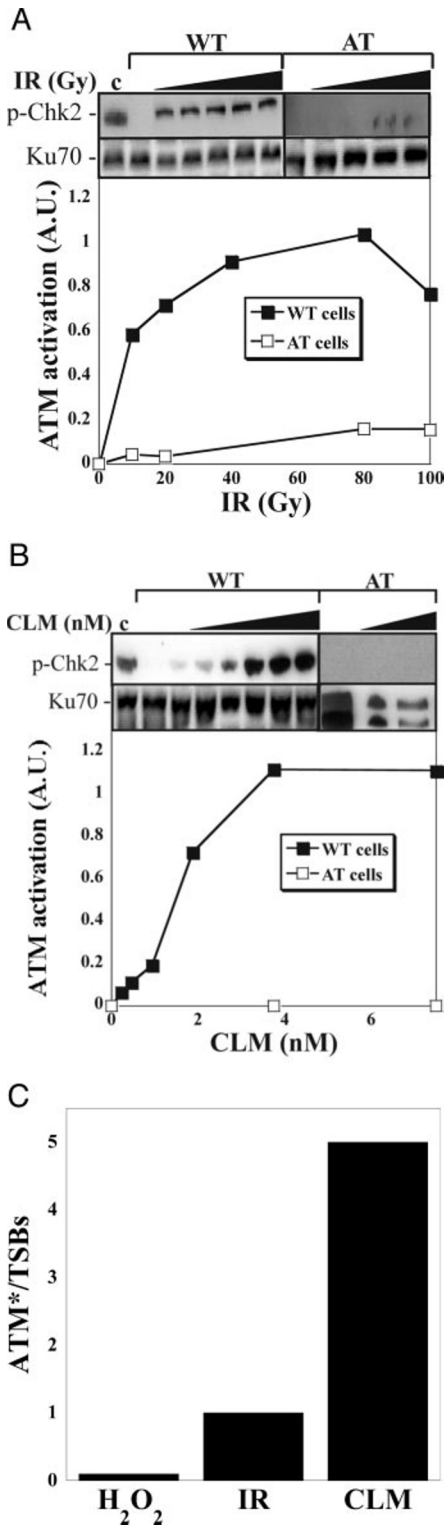

FIG. 6. **ATM activation (*ATM***) by CLM and IR.** Human lymphoblast cells from wild type (*WT*) and AT patients (*AT*) were treated with different concentrations of CLM or IR, as indicated in the figure, at 37 °C for 15 min. WT cells treated with 10 nM CLM for 30 min at 37 °C were used as a control (*c*) to compare Chk2 signals in *A* and *B*. The ATM-dependent phosphorylation was measured by immunoblot using phospho-Chk2 antibody as indicated in the figure. As a control for equal loading, the amount of Ku70 was determined with immunoblot in each sample. The ECL signals from the CLM and IR immunoblots for IR (*A*) or CLM (*B*) were quantified using a digital camera and normalized to the control. The signals from the relevant bands were plotted as a function of the CLM concentration. *Gy*, gray. *A.U.*, arbitrary units. *C*, bar graph of the phosho-Chk2 signals divided with total DNA strand breaks (*TSB*s) determined using the comet assay in the same cells. The values were normalized to the value obtained in IR-treated cells.

concentrations that induce >40,000 SSBs/cell. At this concentration, H_2O_2 did not inactivate ATM or interfere with its ability to recognize DNA damage, because ATM was still activated when DSBs were induced by CLM. CLM-induced strand breaks activated ATM, even at concentrations that induced 300 strand breaks/cell. Based on these findings, we were able to calculate that H_2O_2-induced DNA strand breaks were at least 400-fold less effective in activating ATM than CLM-induced strand breaks. Using the FAR assay, we were not able to detect any DSBs in H_2O_2-treated cells at the highest concentration tested (3 mM), which is in agreement with previous data (37). Because ATM was partially inactivated at 1 mM H_2O_2, we concluded that it was not relevant to perform experiments at 100 mM H_2O_2, which has previously been shown to induce detectable numbers of DSBs (37). Our measurements indicate that H_2O_2 induces over 400,000 SSBs/cell at a concentration of 5 mM. Our assay for DSBs was able to detect DSBs down to 10 gray, a dose that is expected to generate 200–500 DSBs/cell. Assuming that 500 DSBs/cell was the lower detection limit in our FAR assay, we concluded that the percentage of DSBs induced by H_2O_2 must be <0.1%. Apart from the small number of DSBs produced by H_2O_2, the DNA damage distribution and the chemistry of the DNA damage are both very similar to the DNA damage produced by IR (33–35). The fact that ATM is not activated at all by H_2O_2-induced DNA damage indicates that the few DSBs produced by IR do activate ATM. A previous report (39) shows that ATM is activated in response to oxidative stress, including H_2O_2 treatment. In this study, however, the H_2O_2 treatment was prolonged, allowing secondary events such as DNA-replication fork collapse or Nrf2-mediated signals to occur (40).

We also found that cells treated with CLM activated ATM to a higher extent than did IR-treated cells. At similar levels of TSBs, ATM was activated close to 5-fold more efficiently by CLM than by IR. In a previous study (29), we conclude that 30% of all DNA strand breaks induced by CLM are DSBs, whereas the level of DSBs induced by IR is only 2–5%. The level of ATM activation observed in CLM-treated cells therefore correlates closely with the numbers of DSBs induced. Together these data provide strong evidence that ATM is exclusively activated by the few DSBs that are produced by IR.

A recent report (16) indicates that ATM is activated by chromatin changes induced by the chromatin relaxation that occurs when DSBs are induced. As evidence of this "activation at a distance" hypothesis, the authors show ATM activation in response to drugs and hypotonic treatments that have been shown to change chromatin structure but not to induce DNA strand breaks (16). Our data indicate that chromatin relaxation is not likely to be the major activating event. SSBs and DSBs are both capable of relaxing supercoiled DNA, and it is therefore expected that activation of ATM would be observed in response to sufficiently high levels of SSBs. In fact, several reports (27, 28) indicate that full relaxation of chromatin supercoiling in the dihydrofolate reductase locus occurs when SSBs are spaced <45,000 bp apart. It would therefore take roughly 50,000 SSBs to remove all the chromatin supercoiling in a cell. The fact that we did not observe any ATM activation by H_2O_2, even at 40,000 SSBs/cell, indicates that chromatin relaxation cannot be the major mechanism regulating ATM.

Because SSBs fail to activate ATM, it is possible that ATM recognizes DSBs directly. This could indicate that ATM, similar to its homologues, DNA-PKcs and ATR, is guided to DSBs by a DNA-binding cofactor (41–46). DNA-PK might serve as an outstanding example of this scenario. DNA-PKcs binds, similar to ATM, loosely and non-specifically to DNA in the absence of its DNA-binding factor, Ku. Ku is a hollow protein that slides

onto DNA from the end (47). When Ku slides inward on the DNA, it exposes a short DNA-PKcs interacting amino acid sequence that is normally hidden (48). DNA-PKcs then binds cooperatively to the terminal 10 nucleotides of the DNA end and to Ku, resulting in a stable complex that is specifically assembled on DNA ends. In the next step, DNA-PKcs interacts with one of the single-stranded DNA ends at the break to become an active kinase (49). This activation probably occurs when a single-stranded DNA end is inserted into an enclosed channel present in DNA-PKcs (50). It is possible that a similar mechanism applies to ATM. The low resolution structure of ATM indicates that it also contains channels that are able to interact with DNA (51). Purified ATM interacts weakly and non-specifically with DNA and is weakly activated in the presence of any type of DNA or negatively charged polymers, such as heparin sulfate (17, 21). ATM is also specifically retained in foci containing DSBs together with phosphorylated H2AX, indicating that ATM localizes to DSBs in the cell (16). One candidate for the DNA-binding subunit of ATM is the MRN complex, a helicase and nuclease complex required for ATM activation and effective initiation of the DSB signal (19). However, both purified ATM and MRN fail to bind specifically to DNA ends (20). In addition, ATM kinase activity is not specifically stimulated by DNA ends even in the presence of the MRN complex *in vitro* (20). The possible DNA-binding factor for ATM is therefore still unknown.

Another possibility is that chromatin-associated proteins expose new epitopes for protein-protein interaction specifically when the continuity of the DNA helix is broken. These epitopes could serve as a loading point for the MRN complex and ATM. The possibility that ATM interacts with chromatin and not DNA could explain why purified ATM and MRN complex fail to bind specifically to exposed DNA ends.

In conclusion, our data indicate that ATM is activated specifically in response to the DSBs introduced by IR. This finding limits the possible mechanisms of ATM activation in cells and indicates the existence of a DNA-binding subunit that specifically brings ATM to DSBs.

Acknowledgments—We thank Prof. Per Elias for careful reading of the manuscript. We also thank the Swegene Centre for Cellular Imaging at Gothenburg University for the use of imaging equipment.

REFERENCES

1. Shiloh, Y. (2003) *Nat. Rev. Cancer* **3,** 155–168
2. Tounekti, O., Kenani, A., Foray, N., Orlowski, S., and Mir, L. M. (2000) *Br. J. Cancer* **84,** 1272–1279
3. Canman, C. E., Lim, D.-S., Cimprich, K. A., Taya, Y., Tamai, K., Sakaguchi, K., Appella, E., Kastan, M. B., and Siliciano, J. D. (1998) *Science* **281,** 1677–1679
4. Nakagawa, K., Taya, Y., Tamai, K., and Yamaizumi, M. (1999) *Mol. Cell. Biol.* **19,** 2828–2834
5. Banin, S., Moyal, L., Shieh, S.-Y., Taya, Y., Anderson, C. W., Chessa, L., Smorodinsky, N. I., Prives, C., Reiss, Y., Shiloh, Y., and Ziv, Y. (1998) *Science* **281,** 1674–1677
6. Kuhne, M., Riballo, E., Rief, N., Rothkamm, K., Jeggo, P. A., and Lobrich, M. (2004) *Cancer Res.* **64,** 500–508
7. Savitsky, K., Sfez, S., Tagle, D., Ziv, Y., Sartiel, A., Collins, F., Shiloh, Y., and Rotman, G. (1995) *Hum. Mol. Genet.* **4,** 2025–2032
8. Barzilai, A., Rotman, G., and Shiloh, Y. (2002) *DNA Repair* (*Amst.*) **1,** 3–25
9. Lavin, M. F., and Shiloh, Y. (1997) *Annu. Rev. Immunol.* **15,** 177–202
10. Kurz, E. U., and Lees-Miller, S. P. (2004) *DNA Repair* (*Amst.*) **3,** 889–900
11. Burma, S., Chen, B. P., Murphy, M., Kurimasa, A., and Chen, D. J. (2001) *J. Biol. Chem.* **276,** 42462–42467
12. Matsuoka, S., Rotman, G., Ogawa, A., Shiloh, Y., Tamai, K., and Elledge, S. (2000) *Proc. Natl. Acad. Sci. U. S. A.* **97,** 10389–10394
13. Melchionna, R., Chen, X. B., Blasina, A., and McGowan, C. H. (2000) *Nat. Cell Biol.* **2,** 762–765
14. Ahn, J. Y., Schwarz, J. K., Piwnica-Worms, H., and Canman, C. E. (2000) *Cancer Res.* **60,** 5934–5936
15. Kim, S. T., Xu, B., and Kastan, M. B. (2002) *Genes Dev.* **16,** 560–570
16. Bakkenist, C. J., and Kastan, M. B. (2003) *Nature* **421,** 499–506
17. Goodarzi, A. A., and Lees-Miller, S. P. (2004) *DNA Repair* (*Amst.*) **3,** 753–767
18. Lavin, M. F. (2004) *DNA Repair* (*Amst.*) **3,** 1515–1520
19. Uziel, T., Lerenthal, Y., Moyal, L., Andegeko, Y., Mittelman, L., and Shiloh, Y. (2003) *EMBO J.* **22,** 5612–5621
20. Lee, J. H., and Paull, T. T. (2004) *Science* **304,** 93–96
21. Chan, D. W., Son, S.-C., Block, W., Ye, R., Khanna, K. K., Wold, M. S., Douglas, P., Goodarzi, A. A., Pelley, J., Taya, Y., Lavin, M. F., and Lees-Miller, S. P. (2000) *J. Biol. Chem.* **275,** 7803–7810
22. Bromberg, K. D., Burgin, A. B., and Osheroff, N. (2003) *J. Biol. Chem.* **278,** 7406–7412
23. Zhang, Y., Ma, W. Y., Kaji, A., Bode, A. M., and Dong, Z. (2002) *J. Biol. Chem.* **277,** 124–131
24. Zhang, Y., Cho, Y. Y., Petersen, B. L., Bode, A. M., Zhu, F., and Dong, Z. (2003) *J. Biol. Chem.* **278,** 12650–12659
25. Ha, L., Ceryak, S., and Patierno, S. R. (2003) *J. Biol. Chem.* **278,** 17885–17894
26. Nur-E-Kamal, A., Li, T.-K., Zhang, A., Qi, H., Hars, E. S., and Liu, L. F. (2003) *J. Biol. Chem.* **278,** 12475–12481
27. Ljungman, M., and Hanawalt, P. C. (1992) *Proc. Natl. Acad. Sci. U. S. A.* **89,** 6055–6059
28. Ljungman, M., and Hanawalt, P. C. (1995) *Nucleic Acids Res.* **23,** 1782–1789
29. Elmroth, K., Nygren, J., Martensson, S., Ismail, I. H., and Hammarsten, O. (2003) *DNA Repair* (*Amst.*) **2,** 363–374
30. Stiff, T., O'Driscoll, M., Rief, N., Iwabuchi, K., Lobrich, M., and Jeggo, P. A. (2004) *Cancer Res.* **64,** 2390–2396
31. Prise, K. M., Davies, S., and Michael, B. D. (1989) *Int. J. Radiat. Biol.* **55,** 583–592
32. Cantoni, O., Sestili, P., and Cattabeni, F. (1988) *Xenobiotica* **18,** 1481–1487
33. Bradley, M. O., and Erickson, L. C. (1981) *Biochim. Biophys. Acta* **654,** 135–141
34. Massie, H. R., Samis, H. V., and Baird, M. B. (1972) *Biochim. Biophys. Acta* **272,** 539–548
35. Lesko, S. A., Drocourt, J. L., and Yang, S. U. (1982) *Biochemistry* **21,** 5010–5015
36. Lee, M. D., Ellestad, G. A., and Borders, D. B. (1991) *Acc. Chem. Res.* **24,** 235–243
37. Dahm-Daphi, J., Sass, C., and Alberti, W. (2000) *Int. J. Radiat. Biol.* **76,** 667–675
38. Okano, S., Lan, L., Caldecott, K. W., Mori, T., and Yasui, A. (2003) *Mol. Cell. Biol.* **23,** 3974–3981
39. Chen, K., Albano, A., Ho, A., and Keaney, J. F. J. (2003) *J. Biol. Chem.* **278,** 39527–39533
40. Kang, M. I., Kobayashi, A., Wakabayashi, N., Kim, S. G., and Yamamoto, M. (2004) *Proc. Natl. Acad. Sci. U. S. A.* **101,** 2046–2051
41. Zou, L., and Elledge, S. J. (2003) *Science* **300,** 1542–1548
42. Gottlieb, T. M., and Jackson, S. P. (1993) *Cell* **72,** 131–142
43. Sancar, A., Lindsey-Boltz, L. A., Unsal-Kacmaz, K., and Linn, S. (2004) *Annu. Rev. Biochem.* **73,** 39–85
44. Smith, G. C., Cary, R. B., Lakin, N. D., Hann, B. C., Teo, S. H., Chen, D. J., and Jackson, S. P. (1999) *Proc. Natl. Acad. Sci. U. S. A.* **96,** 11134–11139
45. Unsal-Kacmaz, K., Makhov, A. M., Griffith, J. D., and Sancar, A. (2002) *Proc. Natl. Acad. Sci. U. S. A.* **99,** 6673–6678
46. Unsal-Kacmaz, K., Sancar, A., Makhov, A. M., and Griffith, J. D. (2004) *Mol. Cell. Biol.* **24,** 1292–1300
47. Walker, J. R., Corpina, R. A., and Goldberg, J. (2001) *Nature* **412,** 607–614
48. Gell, D., and Jackson, S. (1999) *Nucleic Acids Res.* **27,** 3494–3502
49. Hammarsten, O., DeFazio, L., and Chu, G. (2000) *J. Biol. Chem.* **275,** 1541–1550
50. Leuther, K. K., Hammarsten, O., Kornberg, R. D., and Chu, G. (1999) *EMBO J.* **18,** 1114–1123
51. Llorca, O., Rivera-Calzada, A., Grantham, J., and Willison, K. R. (2003) *Oncogene* **22,** 3867–3874